Sustainable Materials and Technologies 41 (2024) e00990

Contents lists available at ScienceDirect

Sustainable Materials and Technologies

journal homepage: www.elsevier.com/locate/susmat

On the intermolecular interactions and mechanical properties of polyvinyl alcohol/inositol supramolecular complexes

Dewang Wei [a], Yang Fang [a], Lei Liu [b], Jinfeng Dai [a,*], Youming Yu [a], Min Hong [d], Siqi Huo [d], Zhiguang Xu [e], Qianqian Cao [c,*], Pingan Song [d,f,*]

[a] College of Chemistry and Materials Engineering, Zhejiang A & F University, Hangzhou 311300, China
[b] College of Environment and Safety Engineering, Qingdao University of Science and Technology, Qingdao, 266045, China
[c] College of Mechanical and Electrical Engineering, Jiaxing University, Jiaxing 314001, China
[d] Centre for Future Materials, University of Southern Queensland, Springfield 4300, Australia
[e] China-Australia Institute for Advanced Materials and Manufacturing, Jiaxing University, Jiaxing 314001, China
[f] School of Agriculture and Environmental Science, University of Southern Queensland, Springfield 4300, Australia

ARTICLE INFO

Keywords:
Polyvinyl alcohol
Intermolecular interactions
Mechanical properties
Chain movement
Hydrogen-bond cross-link
Coarse-grained model

ABSTRACT

Hydrogen-bond (H-bond) cross-linking has recently been proven a promising strategy for simultaneously improving strength, toughness, and ductility of H-bonded polymers. However, there has been a lack of a fundamental understanding of how H-bond cross-linking works on a molecular level. To fill this knowledge gap, coarse-grained (CG) simulation provides a possibility because of its high computational efficiency and access to longer lengths and time scales. However, existing coarse-grained force fields and potential functions exhibit an inability to accurately describe H-bonded polymer systems. Herein, we report a modified CG model to understand the H-bond crosslinking effect of small molecules, inositol (IN) on polyvinyl alcohol (PVA), with reference to MARTINI 3.0 parameters and empirical data. The simulation results show that incorporating IN molecules results in a significant improvement in the strength, ductility, and toughness of PVA, which is in good agreement with experimental data. Moreover, the modified CG model establishes a close correlation between IN content, water content, tensile rate and glass transition, free volume, chain movement and mechanical properties of PVA. The results show that the yield strength of PVA initially increases and then decreases with the addition of IN. The maximum yield stress of PVA at IN-1.0 is approximately 155 MPa, representing a 33% increase compared to that of PVA. Additionally, the glass transition temperature (T_g) reaches 80.2 °C, ~2.8 °C higher than that of pure PVA. This work develops a modified CG model for understanding intermolecular interactions and mechanical properties of H-bonded polymer systems on a molecular level. This understanding is expected to help expediate the material design and properties optimization of strong and tough polymeric materials.

1. Introduction

Polyvinyl alcohol (PVA), given its high light transmittance, excellent water solubility, stable thermal characteristics, and non-corrosive nature, constitutes an integral component of the polymer matrix [1,2]. Recently, there has been a surge in interest surrounding the study and design of durable PVA materials, primarily to broaden their practical applications across various industries [3,4]. Theoretical and simulation studies have played a key role in the optimization of material properties and understanding the material design [5]. Simulation studies can explain polymer polymerization and weak action mechanisms from the molecular level, such as hydrogen bond (H-bond) and π-π interactions [6,7].

The field of coarse-grained (CG) modeling has been widely adopted to simulate polymer systems of more complex [8,9]. Unlike other atomistic approaches, common CG methods focus on providing a broad, holistic perspective of material categories instead of delving into individual atoms. The key advantage of this approach lies in its computational efficiency, enabling access to longer length and time scales [10]. Furthermore, these methods offer a physical viewpoint that pertains to the entire category of materials under consideration. For example, in the popular universal bead-spring simulation [11,12], the connectivity and

* Corresponding authors.
E-mail addresses: Jinfengdai0601@zafu.edu.cn (J. Dai), qqcao@mail.zjxu.edu.cn (Q. Cao), pingan.song@usq.edu.au (P. Song).

https://doi.org/10.1016/j.susmat.2024.e00990
Received 25 March 2024; Received in revised form 15 May 2024; Accepted 22 May 2024
Available online 25 May 2024

number of beads can be adjusted in obvious ways to describe the basic polymer characteristics and help to reveal the molecular scale behavior of the structure-property relationship of various types of polymer systems. As a molecular dynamic simulation, CG models have been applied to handle the problem of H-bond interactions. Pavel et al. introduced a transferable CG model describing hydrogen-bonded liquids for molecular dynamics simulations of pure methanol liquids [13]. Daniel J et al. developed a new CG model to simulate cellulose chain assembly due to hydrogen bonding [14]. Despite the positive efforts made to describe hydrogen bond interactions via the general CG model, there are still shortcomings of the overly specific experimental protocols that exhibit a limit model to a single chemical system.

The MARTINI CG model [15,16], initially developed for lipid systems, has shown promise in studying polymer Coarse-Grained methods across various reference systems [17]. Due to the simplicity of the MARTINI force field, the reparameterization of each system under study is avoided using a general formula. Features improved interaction balance, new bead types, and the ability to expand to include specific hydrogen bond interactions. The improved model can predict molecular accumulation and interactions more accurately. As described in Martini 3.0, S beads represent four non-hydrogen atoms, which can parameterize PVA. By MARtini3.0 force field, the hydrogen bond capacity was parameterized into Van der Waals interactions to consider the effect of dense hydrogen-bond interactions in terms of H-bond cross-linking changes in polymers. With this foundation, the effects of H-bond interactions can be simulated at low cost, but with high efficiency and accuracy through serving small organic molecules as H-bond cross-linkers [18]. Moreover, the molecular mechanisms also be elucidated, linking the mechanical properties to factors like water content [19] and the glass transition temperature (T_g) [20]. Previous experimental studies exhibit numerous shortcomings in characterizing the microstructure and mechanical properties of PVA/IN [18]. For instance, the experimental methods offer limited information, failing to comprehensively characterize the complex structure of polymer composites. Sample representation might be inadequate, external factors could influence results, and experiments may be costly and time-consuming. Additionally, some methods are destructive, there are limitations on the micro scale, data interpretation poses challenges, and human error may also impact outcomes.

Inositol (IN), as a small molecule polyol, with exceptional water solubility[18], a symmetrical molecular structure, and the presence of six hydroxyl groups in each molecule, is an ideal small molecular cross-linking agent for forming dense hydrogen bonds with PVA chains. Currently, some studies have used techniques such as infrared spectroscopy and X-ray diffraction to investigate how IN forms dense hydrogen bonds with PVA, revealing its unique structural characteristics and intermolecular interaction mechanisms in depth. For example, by preparing PVA/IN composite films with different IN contents, significant improvements in film strength and fracture toughness can be achieved. The optimal IN content is 1 wt%, resulting in a 31% increase in strength, a 250% increase in ductility, and a 4.6-fold increase in fracture toughness. When the IN content is 5 wt%, the fracture toughness is 5.2 times that of pure PVA. Furthermore, in the IN-1.0 system solution, the correlation length (ξ) (16 nm) is the smallest, the relaxation activation energy (Ea) (121.7 KJ/mol) is the largest, and the diffusion coefficient (D) of PVA molecular chains (10^-7.852 cm^2.s^-1) is the smallest. These data provide theoretical basis and practical reference for our paper, which helps to verify or extend the hypotheses of existing studies. Based on these data, the accuracy of the CG model presented in this paper is further validated. However, the mechanism of action of inositol in certain specific cases remains unclear. Further investigation into the interaction of inositol with other factors, such as water content, is warranted. Molecular dynamics (MD) research accurately simulated the dynamic process of dense hydrogen bond formation from a holistic atomistic perspective and detailed factors such as hydrogen bond number and bond length, thereby providing a theoretical foundation for hydrogen bond formation. Nevertheless, due to constraints in time and computational efficiency, a new simulation approach was necessary to address the challenges encountered in the actual process.

Herein, we specifically selected and employed IN to create PVA supramolecular complexes via H-bond cross-linking interactions [21]. Subsequently, through the modified Coarse-Granulation model, the effect of H-bond interaction is analyzed, and the addition of IN significantly increases the number of hydrogen bonds in the PVA system. These results indicate a substantial improvement in the overall mechanical properties of the final PVA/IN complexes, including yield tensile strength, modulus, toughness, and ductility, compared to the original PVA. But excessive IN molecules tend to form hydrogen bonds among molecules themselves, leading to the formation of aggregates or crystals. This in turn results in the plasticization of PVA, causing a decrease in the strength and modulus of the matrix.

2. Coarse-grained model and simulation method

2.1. Construction of coarse-grained model

Construct coarse-grained models of PVA and inositol efficiently using the Martini force field. Delve into the principles and characteristics of the Martini force field to gather relevant information on PVA and IN, including their structures and properties. Employ the 4–1 rule to map PVA, simplifying the force field simulation by not displaying dihedral and non-dihedral angles. Treat the toroidal inositol molecule differently, considering the interaction between bond energy and angular potential energy without including the LJ force in the toroidal molecule. Select appropriate parameters to establish the initial model, then validate and optimize the model through comparison.

Therefore, based on the MARTINI force field, we constructed the PVA polymer chain as a long chain with 100 particles and aimed at capturing fundamental polymer characteristics. It's worth noting that we have not modeled the functional groups participating in hydrogen bonding as distinct entities, such as -OH. Instead, we've employed harmonic oscillator and angular potentials to describe the behavior of these particles [22]. According to Martini3.0, four non-hydrogen atoms are mapped to a bead using the 4–1 mapping rule (Fig. S1). When mapping non-hydrogen atoms to CG beads, several factors are typically considered. Firstly, chemical similarity is prioritized, wherein atoms with akin chemical properties may be assigned to the same CG beads. Secondly, geometric considerations ensure that the relative geometry of the atoms is preserved. This mapping approach can have significant implications on the representation of interactions involving polar molecules and hydrogen bonds. It may alter the overall polarity characteristics of polar molecules and influence their ability to form hydrogen bonds, thereby affecting the formation and stability of intermolecular interactions. Moreover, the strength of these interactions can impact the overall interaction strength between polar molecules and other entities. To comprehensively understand these factors and their impacts, computer simulations are initially employed to study the effects of mapping strategies and compare the outcomes of different approaches. Subsequently, the simulation results are juxtaposed with experimental data for validation.

Since the PVA contains many polar hydroxyl groups, the P bead type, which also represents polar molecules, was chosen in the Martini force field. Considering the polarity, P2 beads were chosen, which were the most consistent with the data, and they had the same size and mass (4 to 1 mapping) [23]. This standard adopted by the parameterization of the force field allows us to ideally split PVA into several beads of the same polarity and then associate these beads with each of them [17,22]. The mapping of coarse-grained beads to atoms is not uniquely defined. If the mapped particle is the same as the particle of the original MARTINI force field, we use the type of standard mapped bead in the MARTINI force field [10]. The mapping between polyvinyl alcohols is shown in Fig. S1a, and this diagram is used to illustrate how we map the coarser

granulation model to the atomic description of PVA. The same chemical part is represented by a bead of the same MARTINI type, using the bead type reported in Fig. S1a to refer to the bead.

IN was selected as a small molecule polyol cross-linker for coarse granulation modeling. The MARTINI force field has a special treatment for circular molecules (usually using 2–1 or 3–1 mappings) [(22)]. As an exception, we consider the interaction with strong hydrogen bonds between molecules and the influence of hydrogen bond interaction on Van der Waals' parameterization, to be consistent with the experimental data and improve the computational efficiency. Using six small (S) microbeads are introduced to simulate the ring compound to capture and map the molecule, as shown in Fig. S1. The particle type of the ring bead was selected according to the free transfer energy of the whole PVA molecule between water and IN, and the model was verified using the free energy [17]. SNd is the type of bead in Martini's field ring. Furthermore, the distance between the IN beads is limited to an equilibrium value of 0.27 nm, considering the stiffness of the molecules. The harmonic oscillator potential between particles also is described. Finally, we evaluated the free energy difference of the candidate torus molecules constructed with different MARTINI types (large polarity and medium polarity) and obtained the best agreement between the SNd bead types and the experimental data.

2.1.1. Establishment of the initial model

Firstly, a 120*120 Å coarse-grained simulation frame was established to carry out uniaxial tensile tests of elastomers and calculate the strain characteristics of elastomers. All PVA chains and small molecule particles do not overlap, the proportion of small molecules in the polymer proportion is expressed as a mass percentage and has topological characteristics that are similar to those of the polymer network synthesized experimentally in the simulation box. In order to obtain more accurate data, the simulation expands the test scale. In the simulation framework, the Monte Carlo method is utilized to generate the periodic remote connection network and establish its basic parameters, such as the number of nodes. Subsequently, nodes are randomly generated, taking into account periodic boundary conditions to ensure network periodicity. Finally, the topology structure and characteristics of the network are analyzed. The process of initializing various IN and water content within the coarse particle model involves several steps. These include identifying the types and characteristics of IN, setting corresponding parameters based on different water content, considering model simplifications and approximations, and verifying the rationality and accuracy of the initialization results. The LAMMPS molecular model builder Moltemplate was used to replicate the repeating units on the x, y and z arrays. Considering the relative positions of the particles, the simulation frame was evenly allocated so that the distance between the particles was equal, and the chain topology of the system was determined. Finally, the coarse-grained model of the PVA-IN was obtained. As shown in Fig. S2, a-f was divided into different inositol contents to initialize the coarse particle model. g-l is divided into initial models with different water contents.

2.2. Coarse-grained force field and its parameterization

Through re-parameterizing the MARTINI 3.0 force field [23], the accuracy of the model in predicting molecular accumulation and interactions in molecular dynamics simulations is improved. This results in improved ability to describe complex systems and handle complex molecular structures and their interactions more effectively. Moreover, the expression of polar molecules is enhanced, allowing for more accurate characterization of their properties. The stability performance of the simulation process is also enhanced, contributing to overall stability improvement. This enhancement aids in improving energy-saving levels, better maintaining energy balance within the system, optimizing computing efficiency, and reducing the consumption of computing resources.

In MARTINI force field, a coarse-grained model of small molecule polyols with ring structure embedded in polymer matrix was established. The Lennard-Jones(LJ)12–6 potential function is used to describe non-bond interactions [24,25]:

$$U_{ij}(r) = 4\epsilon_{ij}\left[\left(\frac{\sigma_{ij}}{r}\right)^{12} - \left(\frac{\sigma_{ij}}{r}\right)^{6}\right] \quad (1)$$

In this potential function, σ_{ij} represents the closest distance between two particles, and ϵ_{ij} represents the strength of the interaction between the particles. Except for two special toroidal ($\sigma = 0.43$ nm) and antifreeze particles, each pair of interactions is assumed to have the same effective size $\sigma = 0.47$ nm.

To describe the strength of the chemical bond in the MARTINI force field, these beads are described by the bond's stretching potential harmonic bond $V_{bond}(R)$ [(25)]:

$$V_{bond}(R) = k_{bond}(R - R_{bond})^2 \quad (2)$$

Equilibrium bond length $R_{bond} = \sigma = 0.47$ nm, bond stretching force constant $R_{bond} = \sigma = 1250\text{kj/mol/nm}^2$, 1/2 is written as a constant. LJ interactions are excluded between bonding particles. The optimization of the equilibrium values and elastic constants of bond lengths and angles depends on the bond and Angle distributions obtained from atomic simulations.

To describe the molecular chain stiffness in MARTINI force field, the stretching potential energy of the bond-Angle $V_{angle}(\theta)$ is described [(25)]:

$$V_{angle}(\theta) = K_{angle}[cos(\theta) - cos(\theta_0)]^2 \quad (3)$$

Equilibrium bond-Angle θ_0=120°, bond-Angle constant K_{angle}=25kkj/mol/rad^2, 1/2 is written to the constant. The LJ interaction between the adjacent particles cannot be ruled out. For the simplicity of the force field, there is no apparent consideration of dihedral angle potential in the standard MARTINI force field.

2.3. Simulation method

In the process of polymer coarse-granulation simulation, noting the simulation of H-bond cross-linking reactions. H-bond cross-linking is a complex dynamic process which coupled with the inherent limitations of the potential function in describing the formation and breakage of H-bonds. Herein, we simplified the expression of the reaction. Both PVA and IN contain hydroxyl groups that form dense H-bonds between and within the molecules. The essence of H-bond cross-linking is that an electrostatic interaction is formed between the hydroxyl group and the hydroxyl group of the polymer chain. The non-bonding interactions between charged beads are also completely described by the Lennard-Jones potential, and the strength of the interaction (i.e. the depth of the well) of the Lennard-Jones potential is used to distinguish the different polarity levels of CG beads [26]. Therefore, we chose to parameterize a large number of hydrogen bond interaction forces formed by PVA and IN crosslinking in Van der Waals interaction to consider the influence of hydrogen bond crosslinking changes. Lennard-Jones (LJ)12–6 potential functions, 12 and 6 represent the range of repulsive hardness and attractive force, respectively, and r-6 is similar to the attractive potential function of general organic molecules, and the effect is better. While r-12 means repulsion, the potential energy is too steep, so you need to adjust the index to adjust the range of gravity and the hardness of the repulsion. The traditional Lennard-Jones potential, usually 10–12 potential, can be used to describe hydrogen bonding more accurately. More information about other forms of describing hydrogen bonding is available on the Molecular Simulation Experiment website. However, due to the limitation of potential function, the current simulation attempts to achieve the approximate effect of hydrogen bond by adjusting the two parameters ϵ_{ij} and σ_{ij}. The LJ potential function describing the parameters of the van der Waals interaction is used to

Table 1
MARTINI force field fitted by modified CG models of PVA, IN and water.

	ϵ_{ij}(kJ/mol) /σ_{ij}(nm)	R_{bond}(kJ/mol/nm^2)/ k_{bond}(nm)	$\theta_0{}^\circ$/K_{angle} (kJ/mol/ rad^2)
PVA	5.0 /0.47	1250/0.47	120°/25
IN	4.5 /0.43	10,000/0.27	
W	5.0 /0.47		

describe the interaction of physical hydrogen bond crosslinking between molecules.

It is known that H-bonds are stronger than van der Waals interactions but weaker than covalent bonds. Depending on the strength of the intermolecular hydrogen bond cross-linking interaction in the experimental data, the physical hydrogen bond ability is considered by changing the polarity or mass of the molecule. The parameters were obtained by fitting the interaction between PVA and IN, and then simulated in the polymer system after obtaining the parameters. MARTINI field parameters of PVA, IN, and water coarse-grained models are refined in Table 1. The atomic parameter information of MARTINI force field is extracted from OPLS-AA, which can be found in the auxiliary material. The atomic simulation results were obtained using the GROMACS 4.0.2 [27] MD software package in NPT integration. Information about the parameters can also be found in references [15, 25, 28]. However, considering the use of an unusual IN mapping scheme IN the system and the selection of SNd beads, we obtained the intermolecular bond energy of IN molecules by verifying the free transfer energy between PVA and IN and water molecules, and achieved the best simulation effect adapted to IN molecules. The calculation shows that R_{bond}=10,000 kJ/mol/nm^2 is more consistent with the experimental results.

The simulation was modeled by complete H-bond crosslinking. However, this model lacks transferability and requires constant re-parameterization when the molecular composition or molecular H-bonding ability changes to deal with van der Waals force and electrostatic interactions. The model can accurately deal with the H-bond cross-linking and stability influence of the PVA-IN structure, to provide feasibility for H-bond cross-linking reaction. The work can build on previously obtained results, while also guiding the effects of chain length, temperature, strain rate, and the number of hydrogen bonds.

The simulation starts with the non-overlapping structure of all polymer chains and ring small molecules in a 120 × 120 Å box. Then, by using the Nose-Hoover thermostat and barometer, the NPT, as a whole, is compressed, and the temperature rises to about 550 K. It is much higher than the glass transition temperature (T_g) and melting point temperature (T_m) of the polymer chain, so the polymer chains are stacked close to each other in the intermediate curly state. When the system relaxes 200,000 steps, whether the average value of the physical quantities concerned, such as temperature and potential energy, converges near the set value, determines whether the system reaches the equilibrium state. After balancing to a uniform density, the simulation system is further balanced under NVT integration to sample the properties of interest. After full equilibrium, to characterize the mechanical properties of the polymer, the isothermal NPT ensemble was also used for cooling treatment, and the temperature was reduced from 550 K to about 298 K, and the PVA and IN molecules were cooled and crystallized. The three-dimensional periodic boundary conditions were adopted in the whole simulation process. The motion equation is integrated with the integration speed of 10 fs and the Verlet algorithm.

Regarding the simulation of uniaxial stretching, the uniaxial tensile deformation of the simulation is to apply anisotropic interactions on the simulation box. The system applies a series of tensile step strains at regular time intervals Δt which causes the equilibrium network to deform at a given strain rate for coupling. By balancing the system and then stretching the box along a uniaxial direction (for example, x). We set the tensile strain rate to 4.0E-5 atm/fs (tensile strain increases by 4.0E-5 units per unit time) with the same strain rate as the experimental data. Meanwhile, the stress in the tensile direction appears as real stress. All molecular dynamics (MD) simulations are performed in large-scale parallel atomic/molecular simulators (LAMMPS).

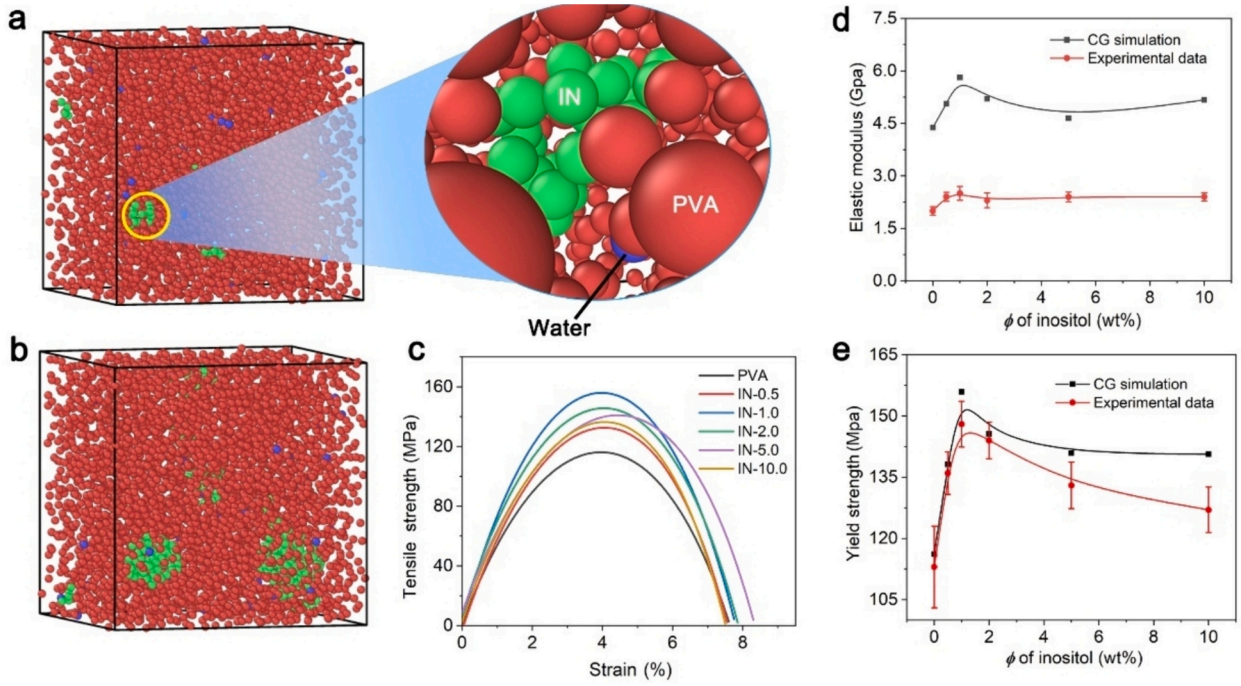

Fig. 1. PVA-IN mixed models with different inositol contents (a) IN-1.0, (b) IN-5.0; (c) PVA-IN mixed plan, small molecules of inositol are agglomerated; (d) Stress-strain diagram of different inositol content; (e) Elastic modulus comparison diagram of different concentrations of inositol between simulation and experimental data; (f) Yield strength comparison diagram of different concentrations of inositol between simulation and experimental data.

Table 2
Comparison of CG-simulated data and experimental data [18].

	CG simulation			Experimental data [18]		
	σ_y (MPa)	E (GPa)	T_g (°C)	σ_y (MPa)	E (GPa)	T_g (°C)
PVA	116.17	4.38	65	113 ± 10	2.0 ± 0.12	77.4
IN-0.5	138.15	5.06	74	136 ± 5.2	2.4 ± 0.13	78.7
IN-1.0	155.94	5.81	78	148 ± 5.6	2.5 ± 0.20	80.2
IN-2.0	145.62	5.20	68	144 ± 4.5	2.3 ± 0.21	77.9
IN-5.0	140.92	4.65	54	133 ± 5.7	2.4 ± 0.14	75.7
IN-10.0	140.64	5.17	45	127 ± 5.6	2.4 ± 0.12	72.7

σ_y, E and T_g are respectively the yield strength, elastic modulus, and glass transition temperature.

3. Results and discussion

3.1. Influence of small molecule concentration of inositol

In our enhanced coarse-size model, we introduced inositol into PVA polymers as a small molecule crosslinker to obtain a homogeneously dispersed composite with a uniform density (Fig. 1). Note that there is a certain relationship between the stable conformation of the molecular system and the initial state of the molecule, and different initializations will cause certain deviations in the simulation data. Therefore, the same initial state of the same molecule is fixed to reduce the deviation of the simulation data. It is found that the content of IN ranging from pure PVA to 10 wt% leads to the corresponding changes of yield strength and elastic modulus of the PVA-IN nanocomposites in the typical tensile stress-strain curve (Fig. 1). With the increase of IN content, the yield strength and elastic modulus of PVA-IN composites are significantly increased. After reaching a peak, it dropped slightly but was still higher than the original PVA sample. This result is in good agreement with the original experimental data [18].

A comparison between the coarse-grained simulation data and experimental data is provided in Table 2, which serves to validate the accuracy of our CG model's parameterization. When the IN content reaches 1.0 wt%, the maximum yield stress of PVA is approximately 155 MPa, representing a 33% increase compared to the original yield strength of 116 MPa. However, as the IN content increases further, both the strength and modulus of PVA decrease. Notably, the maximum toughness is observed at IN-5.0, which is consistent with our experimental findings. In the experimental data, the maximum yield strength at IN-1.0 is approximately 148 MPa, demonstrating a 31% increase compared to the original PVA's yield strength of 113 MPa. Similarly, IN-5.0 exhibits the highest toughness. The addition of IN caused a change in the toughness of the polymer. Concerning tensile toughness, it follows the changing trend of break strain. The elastic modulus and yield strength exhibited similar trends [29,30]. In Fig. 1e and f, we present a comparison between the elastic modulus and yield strength of the CG model and experimental values. The simulated results are consistent with the actual experimental values. However, there is a large deviation in the elastic modulus, which may be caused by many microcracks and voids in the in-situ polymerized PVA-IN, and the mismatch between the test scale and CG simulation. These results collectively underscore the enhancements in strength, stiffness, ductility, and toughness of PVA facilitated by the inclusion of inositol. Furthermore, it highlights the influential plasticizing effect of IN in regulating ductility and toughness.

It should be emphasized that the addition of IN as a small molecule crosslinker to PVA composites has extremely significant effects on the strength, ductility, and toughness of PVA matrix. The addition of IN changes the molecular structure and interaction in PVA matrix, and then affects its strength characteristics [18]. This causes the matrix to have a higher resistance to external forces, making it stronger and more durable. On the other hand, the presence of IN will influence the ductility of PVA matrix. It can increase the deformation capacity of the matrix, making it more flexible when it is stretched or bent, and not easy to break. IN also helps to improve the matrix's ability to absorb and disperse energy, making it more resistant to shock or vibration. Through in-depth analysis of the effect of adding IN as a small molecule crosslinker on PVA matrix, we can better understand the mechanism behind the improvement of mechanical properties. This will help us optimize the material design and further enhance the performance of the PVA matrix to meet the needs of a variety of practical applications.

In this coarse-grained model, the formation and fracture relationships of molecular H-bond crosslinks are determined by continuous re-parameterization according to molecular composition. The crosslinking ability of hydrogen bonds in the PVA-IN system is reflected in the variation of molecular interaction energy. In this work, the molecular interaction energy mainly includes the van der Waals force and the energy contributed by H-bonds. In general, the greater the molecular weight, the greater the van der Waals force. The variation of intermolecular interaction energy is mainly dominated by H-bonding energy. As shown in Fig. 1e, the interaction between PVA can peak at about 1.0 wt % IN content. A turning point also appeared when we calculated the yield strength of 1.0 wt% IN in Fig. 1f. This is mainly because the relatively weaker H-bond between PVA and IN partially replaces the H-bonds between the stronger PVA, resulting in a gradual decrease in the number of PVA-PVA H-bonds, thus weakening the intermolecular interaction [18]. Further observation shows that the interaction between PVA-IN and IN-IN changes linearly. The number of H-bonds between In-ins increases with the increase of IN content. The energy curve of the PVA-IN interaction gradually slows down with the increase of inositol content. Considering the influence of the van der Waals force, the PVA-IN H-bond interaction shows a weakening trend. The variation of the H-bond number in the PVA-IN system is in good agreement with the variation trend of mechanical properties [29,30]. The root reason for the variation of H-bond equivalent crosslinking density with increasing IN contents is explained from the point of view of intermolecular H-bond.

With the increase or decrease of IN concentration, the arrangement of IN molecules in PVA matrix will change significantly. At high concentration, the interaction between molecules will be enhanced, resulting in a closer arrangement of molecules, and their distribution may show a specific regularity. At low concentrations, the distance between the molecules increases and the arrangement is relatively loose. This change in arrangement and distribution will further affect the formation of hydrogen bonds. The formation of hydrogen bonds is closely related to the distance between molecules. When the arrangement and distribution of IN molecules change, the conditions of hydrogen bond formation may also change, which will affect the intermolecular interaction. Changes in molecular interactions may have a key impact on the properties of PVA substrates. For example, changes in hydrogen bonds may affect the stability, solubility, and mechanical properties of the matrix. IN order to further explore the effect of IN concentration on the arrangement and distribution of IN molecules in PVA matrix, hydrogen bond formation and intermolecular interaction, a variety of experimental and theoretical methods are needed. For example, spectroscopy can be used to monitor the arrangement and distribution of molecules; The use of molecular simulation methods is helpful to understand the nature of intermolecular interactions.

When the content of IN is above 1.0 wt%, excessive IN molecules tend to form H-bonds between molecules and eventually form aggregates or crystals, which plasticizes the PVA, resulting in reduced strength and modulus. As the content of small molecule IN increases, varying degrees of agglomeration become evident. In theory, the H-bond cross-linking effect of IN molecules can significantly promote aggregation and crystallization. Polymer crystallinity is a measure of the proportion of crystalline phases within the bulk polymer, closely tied to the ordered arrangement of polymer chains.

Due to the inherent limitations of our coarse-grained model, we are unable to directly calculate the degree of crystallization in the PVA-IN

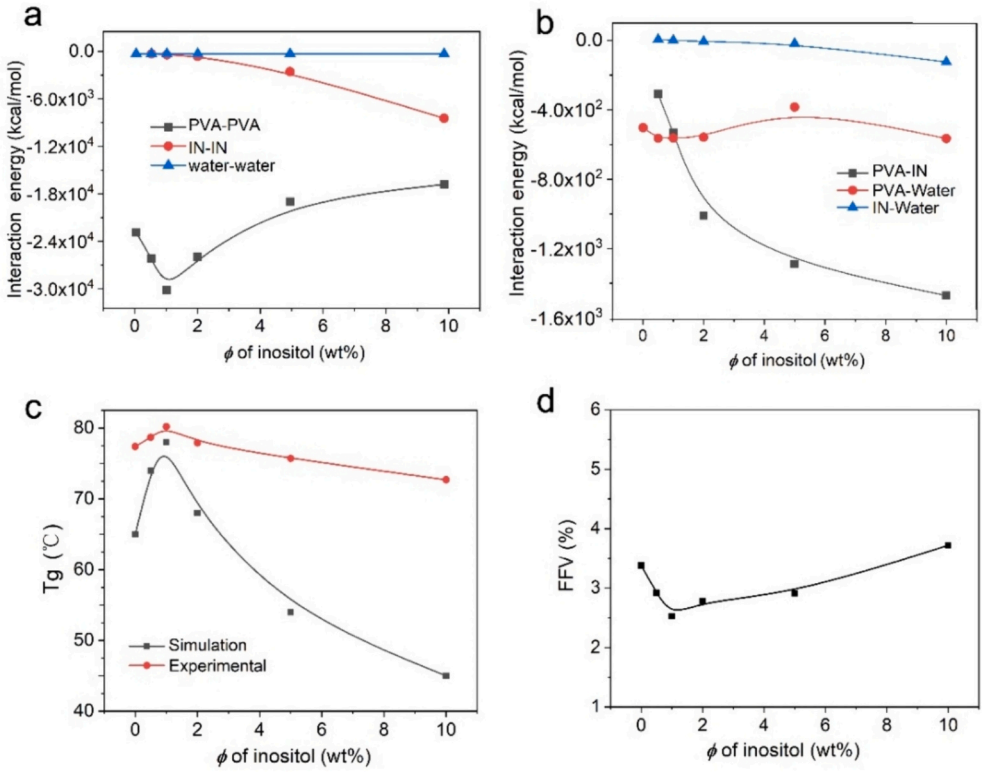

Fig. 2. (a) Interaction energy within the same molecule with different inositol content; (b) The interaction energy between different molecules with different inositol content; (c) T_g comparison between CG models with different inositol content and experimental values [18] and (d) Changes in the free volume fraction of CG models with different inositol content;

system. However, due to the numerous robust H-bonds between PVA and IN, it becomes evident that IN can effectively cross-link PVA chains through multiple H-bonds. Excess IN molecules have a propensity to form larger IN clusters alongside smaller PVA clusters (Fig. S3). To illustrate this, consider the example of 5 wt% IN, where excessive aggregation and substantial crystallization of the IN molecules are apparent. Our model faithfully represents the microstructure and mechanical properties of PVA-IN, offering a comprehensive feasibility analysis for the study of polymer materials.

The T_g is an important characteristic of polymer materials, which defines the glassy region as the rubber region. To calculate the T_g of PVA under different inositol contents, the T_g of PVA polymer material in this paper was determined by the slope change of the specific volumetric temperature curve [31–34]. First, the PVA-IN system is equilibrated at 550 K. Then, the system temperature drops from 550 K to 100 K. Fig. 2c shows a graph of the volume of a polymer system consisting of 40 chains in the system as a function of temperature. The intersection of two linear trend lines fitted to the end of the data gives an estimate of the glass transition temperature [18]. The volume of the polymer will show a turning point near the T_g. The calculated value is about 351 K, which is close to the calculated T_g of 353.2 K.

The T_g of polymer is usually related to the intermolecular interaction, which affects the macroscopic mechanical properties of the polymer system. The addition of IN molecules caused the T_g of PVA to first increase, reach a peak value at 1.0 wt% IN content, and then decrease by increasing of IN content (Fig. 2c). This trend is consistent with the above relationship between yield strength and elastic modulus. This means that there is a close relationship between T_g and mechanical strength and stiffness in PVA-IN systems. The simulation results are in good agreement with the previous experimental values. In Table 1, CG simulation data and experimental data of T_g with different inositol content are also quantified. The trend of CG simulation data and experimental data is highly consistent. However, due to the defects of CG model, there is a large deviation in the projected estimate.

T_g is closely related to the free volume fraction (FFV) of polymer materials [36]. FFV can be used to predict the relative size of free Spaces and the dynamics of polymer matrices. We calculate the FFV at 298 K by the following formula:

$$\mathrm{FFV} = \frac{\mathrm{V} - \mathrm{V}_0}{\mathrm{V}} \tag{4}$$

$$V_0 = 1.3V_W \tag{5}$$

V is the volume, V_0 is the occupied volume and V_W is the van der Waals volume. We analyzed the cross-sectional areas of the cubic volume model in the x, y, and z directions for free volume morphology analysis [37]. We convert the area of the calculated cross-sectional area occupied by the free volume image to the equivalent diameter. Then, the free volume size distribution is obtained by calculating the free volume equivalent diameter [36]. The FFV values we calculated in Fig. 2d are determined using this method.

As shown in Fig. 2d, with an increase of inositol content, FFV first showed a trend of first decreasing and then increasing (Table S1). When the inositol content is 1.0 wt%, FFV reached the lowest level. It is not difficult to understand that the addition of IN molecules makes the PVA produce strong H-bond interactions so that inositol occupies the free space between the polymer chains, thereby reducing FFV. When IN content reaches a certain concentration, excessive H-bonds tend to be generated inside inositol, resulting in large clusters, inhibiting the formation of intermolecular H-bonds, and thereby increasing FFV. The FFV value is mainly determined by the trade-off or competition between these two opposite effects. The results showed that FFV increased with the increase of inositol content.

In order to explain the effect of IN molecules on the kinetic motion of PVA chains, we calculate the mean azimuth shift (MSD) of the polymer complexes [18,19]. The root mean square displacement is used to

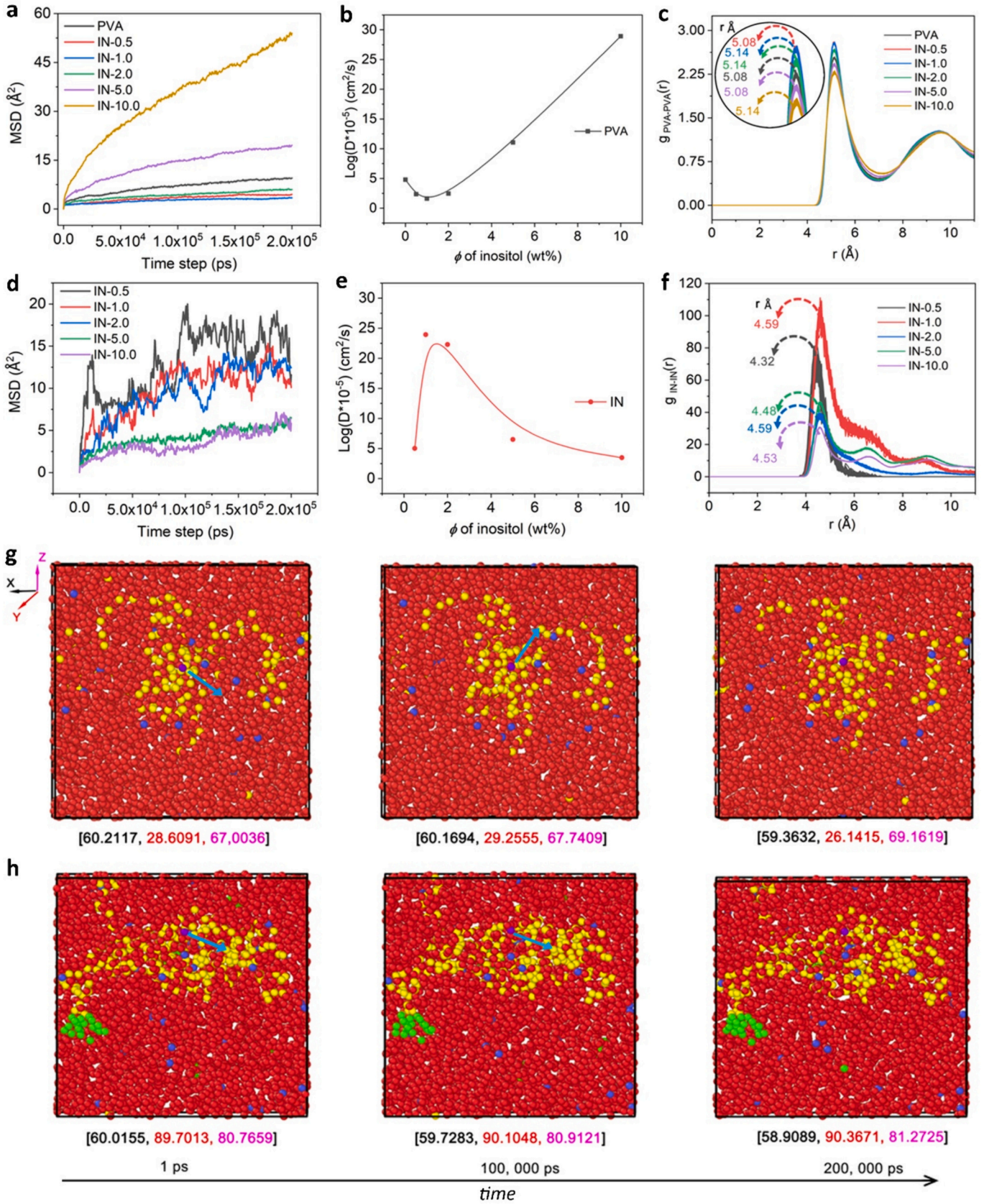

Fig. 3. MSD of (a) PVA and (d) IN in PVA/IN systems with different IN contents; Diffusion coefficient (*D*) curve for (b) PVA chain and (e) IN with varied contents of IN at 298 K; RDF curves for (c) PVA molecular chain and (f) IN with different IN contents; The motion state of a PVA chain (yellow), IN (green), and water (blue) in (g) pure PVA and (h) IN-1.0 system at 1 ps,100,000 ps, 200,000 ps (The blue arrow represents the direction of molecular motion).

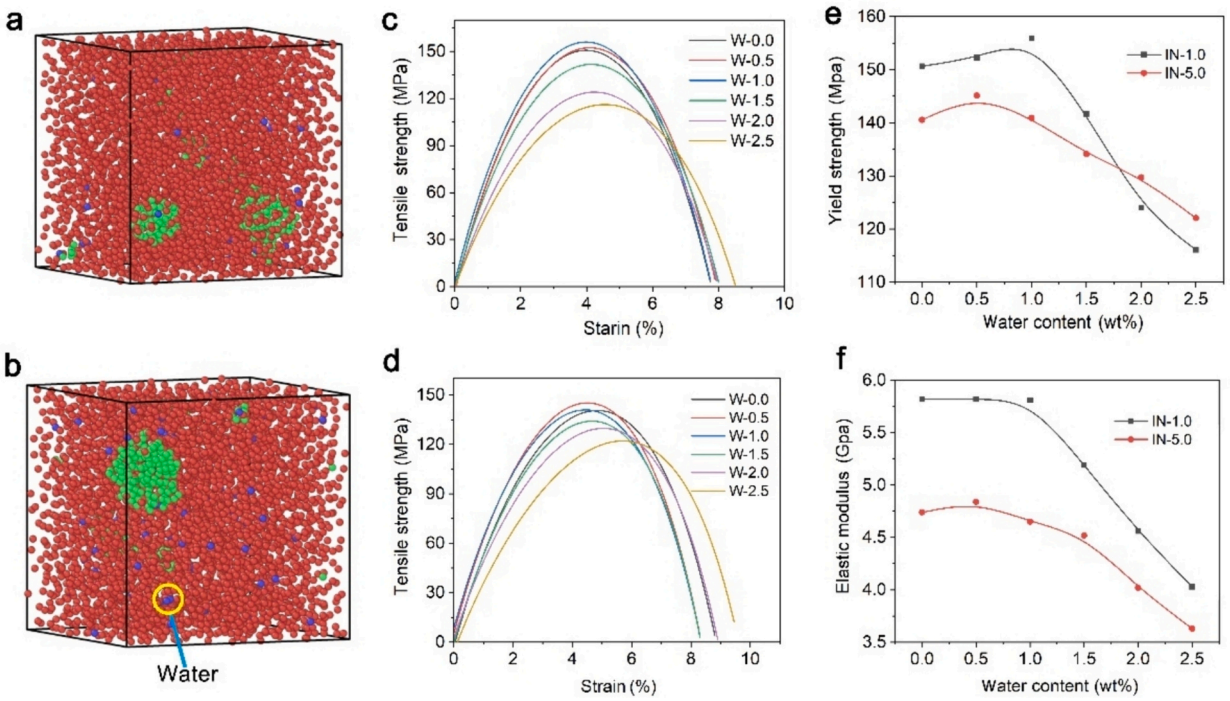

Fig. 4. PVA-IN mixing models with different water contents: (a) W-1.0, (b) W-2.0; Stress-strain diagram of (c) IN-1 and (d) IN-5with different water contents; (e) Yield strength and (f) Elastic modulus of IN-1.0 and IN-5.0 with different water contents.

calculate the mean azimuth shift of the material, and the diffusion velocity of the particles is explained [38]. As the observation time approaches infinity, MSD is proportional to the limiting observation time, and the average of the ensemble at time t is defined by the following formula:

$$MSD = < \frac{1}{N} \Sigma_{i=1}^{N} \left[r_i(t_0 + t) - r_i(t_0)^2 \right] > \tag{6}$$

N is the number of particles, t represents the time, $r_i(t_0 + t) - r_i(t_0)$ is a given particle vector distance traveled over a period of time, $< \frac{1}{N} \Sigma_{i=1}^{N} [r_i(t_0 + t) - r_i(t_0)2] >$ for the balance after the ensemble average. The slope of MSD is the diffusion coefficient RDC, the formula is:

$$D_\alpha = \frac{1}{6N_\alpha} \lim_{t \to \infty} \frac{\mathrm{d}}{\mathrm{d}t} \Sigma_{1=1}^{N_\alpha} [|r_i(t_0 + t) - r_i(t_0)|2] \tag{7}$$

To wit : MSD = $6D_\alpha$t

Figure 3 shows the MSD curves of PVA chain (Fig. 3a) and IN molecules (Fig. 3d). When the content of IN is less than 1.0 wt%, the diffusion rate of PVA decreases first and then increases steadily. In contrast, an opposite trend appears. To further understand the specific details, the diffusion coefficient (D) of the PVA-IN polymer system is calculated, as shown in Fig. 3b and Fig. 3e. With an increase in IN content, the diffusion coefficients of PVA and inositol molecules show a "V" shape trend and reach the minimum and maximum values at 1.0 wt % of IN (or IN-1.0), respectively. This is mainly because of the strong H-bonding interactions between PVA and IN. The results show that the H-bond interactions between PVA and IN seem to decrease with an increase in IN content, due to the H-bonding competition between PVA and IN and themselves. The diffusion rate of PVA system also reaches the highest T_g and yield strength at 1.0 wt% of IN, indicating a balanced H-bond interactions between PVA and IN. Also, we quantify the motion state of a certain polymer chain (yellow chain) at 298 K with pure PVA and IN-1.0 and capture snapshots of 1 ps,100,000 ps and 200,000 ps, respectively (Fig. 3g and Fig. 3h). It can be seen from the coordinates that the diffusion rate of pure PVA is faster than that of IN-1.0, indicating the impact of strong H-bond crosslinking of IN molecules on PVA chains.

Table 3
Yield strength and elastic modulus data for IN-1.0 and IN-5.0.

	IN-1.0		IN-5.0	
	σ_y (MPa)	E (GPa)	σ_y (MPa)	E (GPa)
W-0	150.7	5.82	140.6	4.74
W -0.5	152.3	5.82	145.2	4.84
W -1.0	155.9	5.81	140.9	4.65
W -1.5	141.7	5.19	134.1	4.52
W -2.0	124.0	4.56	129.7	4.02
W -2.5	116.1	4.03	122.1	3.63

σ_y and E are respectively the yield strength and elastic modulus.

In addition, the radial distribution function (RDF) is calculated to reveal the statistical distances between PVA chains and between IN molecules with varied IN contents [18,39]. By observing the RDF curves between PVA chains (Fig. 3c) and IN molecules (Fig. 3f) in Fig. 3, one can see that the peak intensity of RDF curves with different IN contents first increases and then decreases, mainly because IN molecules replace the original intermolecular H-bonds between PVA chains. This result has a similar variation trend with T_g, yield strength, MSD, etc., which further reveals the hydrogen bond interaction between PVA and IN. By observing the interchain distance of PVA chains, when the inositol content increases to 1.0 wt%, the interchain distance of PVA chains and IN molecular chains slightly increases, and then decreases with an increase of IN content, which further proves the strong H-bond interactions between them. In summary, the CG simulation results provide additional evidence for the inhibition effect of IN molecules on the diffusion of PVA chains through H-bond crosslinking.

3.2. *Influence of water content*

Based on the coarse-granulation model, we embarked on an exploration of the influence of water content by introducing varying

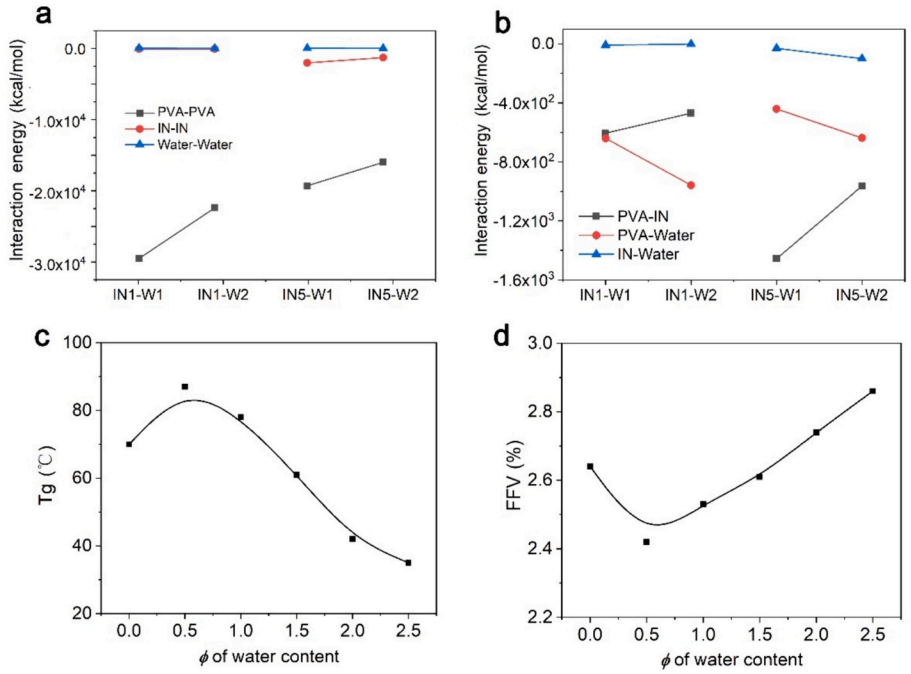

Fig. 5. (a) Intramolecular interaction energy of IN-1.0 and IN-5.0 with different water contents (W-1.0 and W-2.0); (b) Intermolecular interaction energy of IN-1.0 and IN-5.0 with different water contents (W-1.0 and W-2.0); (c) T_g and (d) FFV of IN-1.0 with varied water contents.

quantities of water molecules into the PVA-IN system, allowing the system to equilibrate into a relatively uniform-density mixed model (as depicted in Fig. 4 or Fig. S4). Previous studies have shown that water molecules can significantly determine the macroscopic mechanical properties of polyvinyl alcohol [19]. Through the coarse-grained model of PVA-IN and water molecules, we systematically studied the effect of water content on the mechanical properties of PVA-IN composites. Fig. 4 illustrates the stress-strain curves for IN-1.0 (Fig. 4c) and IN-5.0 (Fig. 4d) with varying water contents, ranging from 0 to 2.5 wt%. Table 3 quantifies the yield strength and elastic modulus data for IN-1.0 and IN-5.0. The yield strength of PVA-IN composites increases first with inceasing water content and then decreases after reaching the peak value. The difference is that IN-1.0 has a peak at 1.0 wt% water content, while IN-5.0 has a peak at 0.5 wt% water content. This is mainly because the addition of water molecules causes the PVA-IN molecules and the H-bonds generated between the water molecules to compete. The elastic modulus of PVA-IN composites (Fig. 4f) showed a similar trend to the yield strength, and the toughness behavior also increased.

Water exerts a significant influence on the mechanical properties of PVA-IN composites. Its presence significantly impacts key mechanical attributes such as strength, ductility, and toughness. Water absorption can compromise the strength and stability of the composite, while simultaneously altering intermolecular interactions, thereby affecting its ductility and toughness. To optimize these effects for specific applications, controlling the moisture content in the composite through appropriate drying or moisture-proof treatments is essential. Additionally, improving the material formulation by adjusting the PVA-to-IN ratio can ensure the desired mechanical properties are achieved under varying moisture conditions. Implementing suitable surface treatment techniques can further enhance the composite's resistance to moisture. Furthermore, mitigating the adverse effects of moisture on the mechanical properties of composite materials involves optimizing processing technology and selecting appropriate methods and conditions. This comprehensive approach aims to minimize the impact of moisture, ensuring the composite maintains its mechanical integrity and performance.

Compared with IN-5.0 content, the yield strength and elastic modulus of 1.0 wt% IN content exhibit a significant decrease as the water content increases. When the water content reaches 2.0 wt%, the yield strength of IN-5.0 is higher than that of IN-1.0. This phenomenon arises from the presence of water molecules, which influence the H-bond interactions within the PVA-IN composite, effectively competing with the H-bonds among PVA chains. To provide a reasonable explanation for this observation, we calculated the molecular interaction energy of two different water contents (W-1.0 and W-2.0) IN-1.0 (Fig. 5a) and IN-5.0 (Fig. 5b). These results show that the interactions between PVA-PVA, PVA-IN and IN-IN can be weakened and the interactions between PVA—W, IN-W, and W—W can be enhanced with an increase of water content. This indicates that the H-bond formed between water and PVA replaces the H-bond between PVA chains after the introduction of water molecules, thus weakening the interaction of PVA chains.

The concentration of IN profoundly influences the intermolecular interactions and mechanical properties of composites. As the concentration of IN increases, molecular interactions change, subsequently impacting the mechanical properties of the composite material. Higher concentrations promote greater molecular binding, thereby enhancing the material's strength and rigidity. The nature of intermolecular interactions directly correlates with mechanical properties, and stronger interactions improve material properties, and different types of interactions yield distinct performance characteristics. However, the presence of water introduces additional complexities to this relationship. Water can modify molecular interactions, such as through hydrogen bonding, leading to changes in material expansion and affecting mechanical properties. Moreover, water may alter the concentration of IN, further influencing mechanical properties. To comprehend this intricate relationship, it is imperative to systematically study the mechanical properties at varying concentrations of IN and analyze the specific influence of water on intermolecular interactions. Such investigations will provide valuable insights for the design and application of composite materials.

However, excessive water content produces more hydrogen bonds between PVA-W and IN-W, or intramolecular H-bonds among water molecules. At the same time, the intramolecular H-bond of PVA chain and the H-bond capacity between PVA-IN and IN-IN are reduced, thus affecting the overall mechanical properties of the PVA-IN system. MD simulation shows that the interaction energy between PVA and water

Table 4
T_g and FFV of IN-1.0 with different water contents.

	T_g (°C)	FFV (%)
W-0	70	2.64
W-0.5	87	2.42
W-1.0	78	2.53
W-1.5	61	2.61
W-2.0	42	2.74
W-2.5	35	2.86

also increases with the increase of water content. This clearly indicates that there is a strong H-bond interaction between PVA and water molecules [40,41]. With the addition of IN, numerous new H-bonds form within the PVA system. The cross-linking of water molecules to the H-bond of PVA chain is affected, ultimately enhancing the yield strength and elastic modulus of PVA. As a result, the yield strength and elastic modulus of IN-5.0 (compared with IN-1.0) tend to be flat at 0–2.5 wt% water content. The study shows that the interaction energy between PVA-W increases greatly, while the interaction energy between the corresponding PVA chain and PVA-IN decreases greatly. This is mainly because most of the intermolecular hydrogen bonds between PVA chains and PVA-IN are replaced by hydrogen bond interactions between PVA and water, while only a small number of hydrogen bonds are formed between water molecules [42].

By establishing volumetric temperature curves (Fig. S4) and FFV calculation (Fig. 2), T_g (Fig. 5c) and FFV (Fig. 5d) of PVA-IN composites with different water content were simulated. The results show that T_g [31–33] of PVA-IN composites decreases with the increase of water concentration, while FFV [35,36] increases with the increase of water concentration, which has also been observed in our previous experiments [19]. In Table 4 (and Table S2), T_g and FFV of different water contents IN In-1.0 are quantified. This phenomenon is mainly due to the volume effect of water molecules, and the addition of water increases the interchain distance and FFV of PVA, thereby increasing FFV [43]. As a result, the FFV showed a steady increase as water contents increased.

Interestingly, T_g and FFV showed the opposite trend when the water content was 0.5 wt%. On one hand, the moisture content within 1.0 wt% of the selected sample has a small overall impact, and the simulation and prediction results may have a large deviation. On the other hand, the true FFV value of PVA cannot be predicted at low water content. This can be explained by the fact that the Fox-Flory theory assumes that FFV is a constant when measured below the T_g of the polymer [18]. The simulation cannot accurately simulate the results of low content.

To further observe the influence of the presence of water molecules on the PVA chain and IN diffusion kinetics [44,45]. As shown in Fig. 6, we calculate the MSD curves of PVA and IN (Fig. S5) for two kinds of IN contents under different water contents. The increase of water content leads to the acceleration of the diffusion of PVA chains (Fig. 6a) and IN (Fig. S5). Interestingly, the diffusion rate of 1.0 wt% of IN decreases at 2.0 wt% of water. This is presumably because when inositol content is low, the increase of water molecules can weaken the H-bond interactions between PVA and IN, resulting in a faster diffusion rate. The diffusion trends of PVA and IN (Fig. S5) in Fig. 6b are reflected by their diffusion coefficient values as a function of water contents. At a low water content, water molecules are confined to the PVA-IN chain due to strong hydrogen bond interactions between molecules. As the water content increases, the water molecule increases the interchain distance between the PVA chains and IN (Fig. S5), thus providing more free space for the water molecule to diffuse. The intermolecular H-bonds between the PVA-IN chains are partially replaced by the H-bonds between PVA and water. A further increase in water contents also leads to a decrease in the free volume of the PVA system, thus reducing the space for the

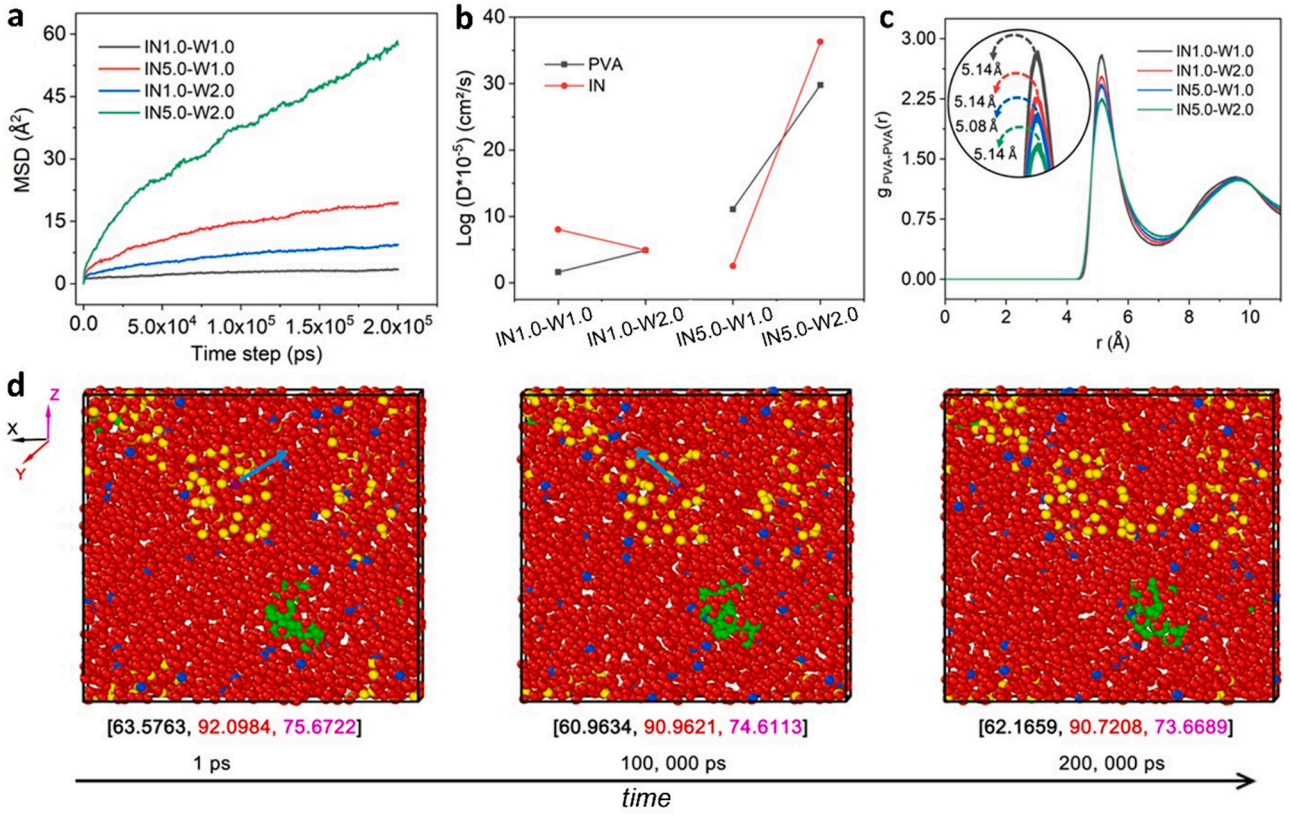

Fig. 6. (a) MSD of PVA under two kinds of IN with different water content; (b) the plot of diffusion coefficient (*D*) with water content of two kinds of IN at 298 K; (c) RDF curves IN-1.0 and IN-5.0 with different water content; (d) Motion states of a PVA chain (yellow), IN (green), and water molecule (blue) in IN1.0-W2.0 system at 1 ps, 100,000 ps, 200,000 ps. (The blue arrow represents the direction of molecular motion).

Table 5
Simulated yield strength and elastic modulus of IN-1.0 and IN-5.0 at different tensile strain rates.

	IN-1.0		IN-5.0	
Strain rate (Atm/fs)	σ_y (MPa)	E (GPa)	σ_y (MPa)	E (GPa)
4.0*10–4	107.3	4.42	97.6	3.55
5.0*10–4	155.9	5.81	140.9	4.65
6.0*10–4	208.9	7.15	189.6	5.71
7.0*10–4	263.9	8.42	242.0	6.73

σ_y and E are respectively yield strength and elastic modulus.

diffusion of PVA chains. As the water content further increases, the diffusion of PVA chains accelerate again due to the gradual increase of FFV and the lubrication of the water clusters. Compared with IN-1.0-W1.0 (Fig. 3h), the diffusion rate of PVA chains in IN-1.0-W2.0 is faster (Fig. 6d), which further verifies that water molecules affect H-bond crosslinking, and thus affect the chain dynamics of PVA chains.

Meanwhile, we calculate the radial distribution function (RDF) of PVA with varied IN contents and two different water contents to further study the influence of water contents on the diffusion of PVA chains [19,43]. The simulation calculates the PVA (Fig. 6c) and the RDF within the IN (Fig. S5) molecules of two IN contents under different water contents. With the increase of water contents, the interchain distance of PVA molecules slightly increases. This is mainly due to strong H-bond interactions between PVA, IN and water molecules, and a small volume of water molecules occupies the free space of molecular chains, thereby increasing the interchain distance. There is a small difference in the peak intensity of different water content in the system in the CG models (Fig. 6c), indicating a slight difference in intermolecular interactions in these systems.

3.3. Influence of tensile strain rate

Compared with the experimental data, the yield strength and elastic modulus of the simulated polymers were similar at the same strain rate (see Fig. 1, Table 5). The experimental simulation value of PVA-IN materials strongly depends on the tensile rate during the tensile experiment, and high tensile rate usually leads to an increase of the yield strength and elastic modulus of PVA [46,47]. Our study clearly shows the effect of strain rate on the uniaxial tensile behavior of elastic PVA-IN composites. As shown in Fig. 7, we performed tensile simulation under the environmental conditions of uniform strain rates at 4.0E-4, 4.0E-5, 4.0E-6 and 4.0E-7 atm/fs and calculated the stress-strain curves of IN-1.0 (Fig. 7a) and IN-5.0 (Fig. 7b) respectively. The mechanical properties vary at different strain rates. As the tensile strain rate increases, the elastic modulus (see Fig. 7c) and yield strength (see Fig. 7d) also increase. The yield strength and elastic modulus of IN-1.0 and IN-5.0 at different tensile strain rates are presented in Table 4. When the strain rate is 4.0E-4 atm/fs, the yield strength and elastic modulus of IN-1.0 are 107.26 MPa and 4.418GPa. When the strain rate reaches 4.0E-7 atm/fs, the yield strength and elastic modulus are as high as 263.94 MPa and 8.422GPa. These findings indicate that PVA-IN composites exhibit significant strain rate sensitivity. At high strain rates, the stress-strain behavior of PVA-IN composites gradually increases. Thus, at high strain rates, a detailed understanding of the material's overall mechanical response, including its load-bearing capacity, can be achieved. By elucidating its deformation characteristics, including deformation modes and rates, the energy absorption and dissipation mechanisms of PVA-IN composites can be revealed.

The elastomer properties of PVA-IN composites mainly include high elasticity, good flexibility, and excellent fatigue resistance. Its potential applications in flexible and elastic materials include wearable devices, cushioning materials and sealing materials. These characteristics change differently at different strain rates. High strain rates may reduce the elasticity and flexibility of the elastomer, affect the fatigue resistance, shorten the fatigue life and accelerate the response speed of the material.

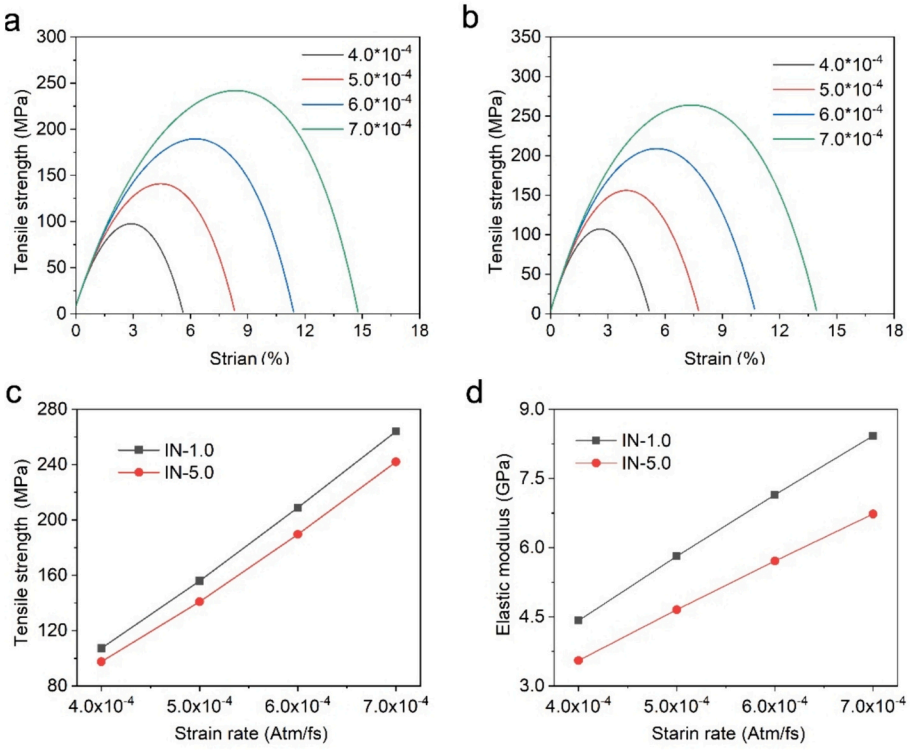

Fig. 7. (a) Stress-strain curves of IN-1.0 at different stretching rates Scheme; (b) Stress-strain curves of IN-5.0 at different stretching rates Scheme; (c) Elastic modulus of IN-1.0 and IN-5.0 at different stretching rates; (d) Yield strength of IN-1.0 and IN-5.0 at different stretching rates.

These studies are conducive to optimizing the properties of the composite to meet the needs of various applications.

The mechanical response of elastomer materials is highly dependent on rate and pressure and exhibits stress-strain nonlinear behavior. In the range of simulated strain rates, the stiffness of PVA-IN composites changes significantly. In the range of simulated strain rates, the stiffness of PVA-IN composites changes significantly; the toughness behavior increases, and the rubber behavior persists at high strain rates. This result is consistent with the well-known effect of strain rate on elastomers, that is, the stiffness of elastomers is directly related to the strain rate [48]. Thus, the initial modulus is largely dependent on the rate of stretching.

4. Conclusions

This work systematically explores how IN molecules impact intermolecular interactions, chain dynamics, and mechanical properties of PVA through H-bond cross-linking effects of IN by using a modified coarse-grained (CG) simulation model. Because of strong H-bonding interactions between IN and PVA, the addition of IN to the model significantly enhances the mechanical properties (strength and modulus) of PVA. Meanwhile, both ductility and toughness also experience notable improvements, indicating that the H-bond cross-linking effect of IN has a significant impact on the microstructure and mechanical properties of PVA, which is in good agreement with previous experimental results. Additionally, the modified CG model establishes a close correlation between the water content, tensile rate, T_g, and free volume of PVA and its mechanical properties. It is the strong H-bond interactions among PVA, IN, and water that determine the microstructure and mechanical performances of PVA/IN molecular complexes. This work pioneers a modified CG model for better understanding the intermolecular interactions and mechanical properties of H-bonded polymeric materials on a molecular level.

CRediT authorship contribution statement

Dewang Wei: Writing – original draft, Formal analysis, Data curation, Conceptualization. **Yang Fang:** Methodology, Investigation. **Lei Liu:** Investigation, Formal analysis. **Jinfeng Dai:** Writing – review & editing, Supervision. **Youming Yu:** Supervision, Funding acquisition. **Min Hong:** Writing – review & editing. **Siqi Huo:** Writing – review & editing. **Zhiguang Xu:** Writing – review & editing. **Qianqian Cao:** Writing – review & editing, Supervision, Methodology, Formal analysis. **Pingan Song:** Writing – review & editing, Supervision, Methodology, Funding acquisition, Conceptualization.

Declaration of competing interest

The authors declare that they have no known competing financial interests or personal relationships that could have appeared to influence the work reported in this paper.

The author is an Editorial Board Member/Editor-in-Chief/Associate Editor/Guest Editor for [Journal name] and was not involved in the editorial review or the decision to publish this article.

The authors declare the following financial interests/personal relationships which may be considered as potential competing interests:

Data availability

No data was used for the research described in the article.

Acknowledgements

This work is financially supported by the National Natural Science Foundation of China (Grant No. 51873196), and the Australian Research Council (Grant Nos. FT190100188, LP220100278, DP240102628, DP240102728).

Appendix A. Supplementary data

The Supporting Information is available free of charge on the ACS Publications website. The coarse-granulation models of PVA/IN complexes with varied inositol contents and water contents were improved. The coarse granulation models of various PVA with varied inositol and water contents were improved. OVITE software was used to visualize and observe the model and simulation results in detail. The fitting process is described in detail in the figure, and the estimated T_g is obtained. The free volume fraction of different inositol contents and the data comparison of two inositol contents with different water contents are listed.

References

[1] J. Jalvandi, M. White, Y. Gao, Y.B. Truong, R. Padhye, I.L. Kyratzis, Polyvinyl alcohol composite nanofibres containing conjugated levofloxacin-chitosan for controlled drug release, Mater. Sci. Eng. C Mater. Biol. Appl. 73 (2017) 440–446.
[2] A. Rafique Zia, K. Mahmood, M. Zuber, S. Tabasum, S. Rehman, Chitosan functionalized poly(vinyl alcohol) for prospects biomedical and industrial applications, a review, Int. J. Biol. Macromol. 87 (2016) 141–154.
[3] P.A. Song, H. Wang, High-performance polymeric materials through hydrogen-bond cross-linking, Adv. Mater. 32 (2020) 1901244.
[4] Y.N. Chen, L. Peng, T. Liu, Y. Wang, S. Shi, H. Wang, Poly(vinyl alcohol)-tannic acid hydrogels with excellent mechanical properties and shape memory behaviors, ACS Appl. Mater. Interfaces 8 (2016) 27199–27206.
[5] C. Wu, W. Xu, Atomistic simulation study of absorbed water influence on structure and properties of crosslinked epoxy resin, Polymer 48 (2007) 5440–5448.
[6] X. Shen, L. Cao, Y. Liu, J. Dai, X. Liu, J. Zhu, S. Du, How does the hydrogen bonding interaction influence the properties of Polybenzoxazine? An experimental study combined with computer simulation, Macromolecules 51 (2018) 4782–4799.
[7] Y. Tan, Y. Song, Q. Zheng, Hydrogen bonding-driven rheological modulation of chemically reduced graphene oxide/poly(vinyl alcohol) suspensions and its application in electrospinning, Nanoscale 4 (2012) 6997–7005.
[8] W. Xu, K. Nitin, Hansoge, S. Xu, F.R. Phelan Jr., Keten Sinan, J.F. Douglas, Energy renormalization for coarse-graining polymers having different segmental structures, Sci. Adv. 5 (2019) eaav4683.
[9] J. Song, D.D. Hsu, K.R. Shull, F.R. Phelan Jr., J.F. Douglas, W. Xia, et al., Energy renormalization method for the coarse-graining of polymer viscoelasticity, Macromolecules 51 (2018) 3818–3827.
[10] A. Arora, T.S. Lin, B.D. Olsen, Coarse-grained simulations for fracture of polymer networks, stress versus topological Inhomogeneities, Macromolecules 55 (2021) 4–14.
[11] G.G. Vogiatzis, G. Megariotis, D.N. Theodorou, Equation of state based slip spring model for entangled polymer dynamics, Macromolecules 50 (2017) 3004–3029.
[12] HP Hsu, K. Kremer, Efficient equilibration of confined and free-standing films of highly entangled polymer melts, J. Chem. Phys. 153(2020) 144902.
[13] P.A. Golubkov, J.C. Wu, P. Ren, A transferable coarse-grained model for hydrogen-bonding liquids, Phys. Chem. Chem. Phys. 10 (2008) 2050–2057.
[14] Z. Wu, D.J. Beltran-Villegas, A. Jayaraman, Development of a new coarse-grained model to simulate assembly of cellulose chains due to hydrogen bonding, J. Chem. Theory Comput. 16 (2020) 4599–4614.
[15] S.J. Marrink, A.H. de Vries, A.E. Mark, Coarse grained model for semiquantitative lipid simulations, J. Phys. Chem. 108 (2004) 750.
[16] S.J. Marrink, H.J. Risselada, S. Yefimov, D.P. Tieleman, A.H. de Vries, The MARTINI force field: coarse grained model for biomolecular simulations, J. Phys. Chem. 111 (2007) 7812.
[17] G. Rossi, I. Giannakopoulos, L. Monticelli, N.K.J. Rostedt, S.R. Puisto, C. Lowe, et al., A MARTINI Coarse-grained model of a thermoset polyester coating, Macromolecules 44 (2011) 6198–6208.
[18] L.J. Li, X.D. Xu, P.A. Song, Q. Cao, X. Qiao, Z. Xu, Y. Yang, C. Zuo, H. Wang, Insights into the hydrogen-bond cross-linking effects of small multiamine molecules on physical and mechanical properties of poly(vinly alcohol) by molecular dynamics simulations, Model. Simul. Mater. Sci. Eng. 29 (2021) 035012.
[19] L.J. Li, X.D. Xu, L. Liu, P.A. Song, Q. Cao, Z.G. Xu, Z.P. Fang, H. Wang, Water governs the mechanical properties of poly(vinyl alcohol), Polymer 213 (2021) 123330.
[20] J. Choi, S. Yu, S. Yang, M. Cho, The glass transition and thermoelastic behavior of epoxy-based nanocomposites: a molecular dynamics study, Polymer 52 (2011) 5197–5203.
[21] W.W. Niu, Y.L. Zhu, R. Wang, Z.Y. Lu, X.K. Liu, J.Q. Sun, Remalleable, healable, and highly sustainable supramolecular polymeric materials combining superhigh strength and ultrahigh toughness, ACS Appl. Mater. Interfaces 12 (2020) 30805–30814.
[22] R. Alessandri, F. Grunewald, S.J. Marrink, The Martini model in materials science, Adv. Mater. 33 (2021) e2008635.
[23] S. Mahajan, T. Tang, Martini coarse-grained model for polyethylenimine, J. Comput. Chem. 40 (2019) 607–618.

[24] P.C.T Souza, R. Alessandri, J. Barnoud, S. Thallmair, I. Faustino, F. Grunewald, al. et, Martini 3.0: a generalpurpose force field for coarse-grained molecular dynamics, Nat. Methods 18(2021) 382–388.
[25] S.J. Marrink, H.J. Risselada, S. Yefimov, D.P. Tieleman, B. Vries, ADJTjopc, The MARTINI force field: Coarse grained model for biomolecular simulations, J. Phys. Chem. B. Condensed 27 (2007) 111.
[26] C. Paulo, T. Souza, Riccardo Alessandri, Jonathan Barnoud, Sebastian Thallmair, Ignacio Faustino, Fabian Grünewald, Ilias Patmanidis, Haleh Abdizadeh, Bart M. H. Bruininks, Tsjerk A. Wassenaar, Peter C. Kroon, Josef Melcr, Luca Monticelli, Xavier Periole, D. Peter Tieleman, H. Alex, de Vries, Siewert J. Marrink, Martini 3: a general purpose force field for coarse-grained molecular dynamics, Nat. Methods 18 (2021) 382–388.
[27] E. Lindahl, B. Hess, D. van der Spoel, Gromacs 3.0: A package for molecular simulation and trajectory analysis, J. Mol. Model. 7 (2001) 306–317.
[28] S.O. Yesylevskyy, L.V. Schafer, D. Sengupta, S.J. Marrink, MJPCB Levitt, Polarizable Water Model for the Coarse-Grained MARTINI Force Field, University of Groningen vol. 6(2013) e1000810.
[29] P.A. Song, Z.G. Xu, Q.P. Guo, Bioinspired strategy to reinforce PVA with improved toughness and thermal properties via hydrogen-bond self-assembly, ACS Macro Lett. 2 (2013) 1100–1104.
[30] P.A. Song, Z.G. Xu, Y. Lu, Q.P. Guo, Bio-inspired hydrogen-bond cross-link strategy toward strong and tough polymeric materials, Macromolecules 48 (2015) 3957–3964.
[31] D. Hossain, M.A. Tschopp, D.K. Ward, J.L. Bouvard, P. Wang, M.F. Horstemeyer, Molecular dynamics simulations of deformation mechanisms of amorphous polyethylene, Polymer 51 (2010) 6071–6083.
[32] C. Wu, Cooperative behavior of poly (vinyl alcohol) and water as revealed by molecular dynamics simulations, Polymer 51 (2010) 4452–4460.
[33] K. Devendra, K. Mrignaini, D.G. Alka, Synthesis and characterization of novel cyclotriphosphazene-containing polys (ether imide), Polymer 34 (1993) 3025–3029.
[34] H. Takeuchi, R.J. Roe, Dynamic mechanical analysis, a practical introduction, second edition, J. Chem. Phys. 94 (1991) 7458e65.
[35] M. Schmidt, Macroscopic volume and free volume of polymer blends and pressure -densified, Polymers 91 (2000) 7178–7197.
[36] K. Chang, C. Tung, K. Wang, K.L. Tung, Free volume analysis and gas transport mechanisms of aromatic polyimide membranes, a molecular simulation study, J. Phys. Chem. 113 (2009) 9821–9830.
[37] X.Y. Wang, D. Roy, J. Hyuck Raharjo, B.D.Y. Lu Lee, I.C. Freeman Sanchez, Molecular simulation and experimental study of substituted polyacetylenes, fractional free volume, cavity size distributions and diffusion coefficients, J. Phys. Chem. 110 (2006) 12666–12672.
[38] Y. Li, M. Kröger, W.K. Liu, Nanoparticle effect on the dynamics of polymer chains and their entanglement network, Phys. Rev. Lett. 109 (2012) 118001.
[39] Y. Fang, T. Yue, S. Li, Z. Zhang, J. Liu, L. Zhang, Molecular dynamics simulations of self-healing topological copolymers with a comblike structure, Macromolecules 54 (2021) 1095–1105.
[40] P. Sappidi, U. Natarajan, Factors responsible for the aggregation behavior of hydrophobic polyelectrolyte PEA in aqueous solution studied by molecular dynamics simulations, J. Mol. Graph. Model. 04 (2017) 306–315.
[41] J. Kleinen, W. Richtering, Rearrangements in and release from responsive microgel-polyelectrolyte complexes induced by temperature and time, J. Phys. Chem. 115 (2011) 3804–3810.
[42] P.A. Song, Z.G. Xu, Y. Lu, Q.P. Guo, Bioinspired strategy for tuning thermal stability of PVA via hydrogen-bond crosslink, Compos. Sci. Technol. 118 (2015) 16–22.
[43] M.L. Connolly, Solvent-accessible surfaces of proteins and nucleic acids, Science 221 (1983) 709–713.
[44] I. Mora-Barrantes, A. Rodríguez, L. Ibarra, L. Gonzlez, J.L. Valentín, Overcoming the disadvantages of fumed silica as filler in elastomer composites, J. Mater. Chem. 21 (2011) 7381–7392.
[45] B. Qiao, X. Zhao, D. Yue, L. Zhang, S. Wu, A combined experiment and molecular dynamics simulation study of hydrogen bonds and free volume in nitrile-butadiene rubber/hindered phenol damping mixtures, J. Mater. Chem. 22 (2012) 12339–12348.
[46] B.M. Tymrak, M. Kreiger, J.M. Pearce, Mechanical properties of components fabricated with open-source 3-D printers under realistic environmental conditions, Mater. Des. 58 (2014) 242–246.
[47] P. Striemann, L. Gerdes, D. Huelsbusch, M. Niedermeier, F. Walther, Interlayer bonding capability of additively manufactured polymer structures under high strain rate tensile and shear loading, Polymer 48 (2022) 25673–27216.
[48] H.M.C.C. Somarathna, S.N. Raman, D. Mohotti, A.A. Mutalib, K.H. Badri, Rate dependent tensile behavior of polyurethane under varying strain rates, Constr. Build. Mater. 254 (2020) 119203.